

Gregory P. Johnston*,****, Prabhat Tiwari*, Donald J. Rej*, Harold A. Davis*, William J. Waganaar*, Ross E. Muenchhausen*, David Tallant**, Regina L. Simpson**, David B. Williams***, and Xiamei Qui****

*Los Alamos National Laboratory, Los Alamos, New Mexico 87545

**Sandia National Laboratory P. O. Box 5800, Albuquerque, New Mexico 87185-0343

***Department of Metallurgy & Materials Engineering, Lehigh University, Bethlehem, Pennsylvania, 18015-3195

****Department of Chemical Engineering, University of New Mexico/Center for Micro-Engineered Ceramics, Albuquerque, New Mexico 87131

Conf-931108-51

ABSTRACT

Diamond-like carbon films were prepared by high intensity pulsed ion beam ablation of graphite targets. A 350 keV, 35 kA, 400 ns pulse width beam, consisting primarily of carbon ions and protons, was focused onto a graphite target at a fluence of 15-45 J/cm². Films were deposited onto substrates positioned in an angular array from normal to the target to 90° off normal. Deposition rates up to 30 nm per pulse, corresponding to an instantaneous deposition rate greater than 1 mm/sec, have been observed. Electrical resistivities between 1 and 1000 ohm·cm were measured for these films. XRD scans showed that no crystalline structure developed in the films. SEM revealed that the bulk of the films contain material with feature sizes on the order of 100 nm, but micron size particles were deposited as well. Both Raman and electron energy loss spectroscopy indicated significant amounts of sp³ bonded carbon present in most of the films.

INTRODUCTION

Diamond-like carbon (DLC) is amorphous carbon with some properties similar to those of crystalline diamond. Compared to graphite, DLC is harder, has a higher electrical resistance, is more transparent (with optical band gap between 0.5 and 2.0 eV), and more chemically resistant.¹ In DLC only a percentage of the carbon (C) atoms are sp³ bonded, the remainder being mostly sp² bonded with some sp¹ possible. DLC with up to 85% sp³ bonded C has been reported.² The physical properties of DLC vary according to the distribution of sp³ and sp² bonding configurations.³ These properties make DLC an attractive candidate for wide variety of applications, including high transmission optical coatings, hard coatings for cutting tools, and low friction films for aerospace components.⁴ The wide optical band gap of these amorphous films can be employed as the active material for electroluminescent flat panel displays.⁵ DLC is also a useful field-emitter because of its thermal stability and low work function, making it a candidate for field emissive displays (FEDs).⁶

A variety of physical vapor deposition techniques have been used to deposit DLC films, including cathodic arc, pulsed laser deposition (PLD), direct ion beam deposition, ion beam sputtering, and magnetron sputtering.² All of these indicate that deposition of unhydrogenated DLC requires the depositing species to be energetic. DLC films produced by PLD (at $\lambda=248$ nm) are obtained with laser power densities of $\sim 10^8$ W/cm² on graphite targets.^{2,7-9} The diamond like character of these films not only depends on the kinetic energies of the incident carbon atoms and ions, but also on the substrate thermal diffusivity and temperature. The highest sp³ fraction DLC films are obtained from an energetic flux of greater than 10 eV/atom, which is deposited onto cold

JOHNSTON

This work was supported by the United States Department of Energy under Contract DE-AC04-94AL85000.

MASTER

DISTRIBUTION OF THIS DOCUMENT IS UNLIMITED

YR

substrates (77K) to enhance the quench rate.⁸ With conventional ion beam deposition, DLC has been directly deposited at room temperature using 40 eV carbon ions.¹⁰ A practical limitation of these PVD techniques is the low deposition rates. Typically, these rates are less than a few $\mu\text{m}/\text{hr}$ even on small ($<10 \text{ cm}^2$) substrates.

Here, we report on high intensity pulsed ion beam deposition (HIPIBD) of DLC. This technique has been previously investigated for deposition of polycrystalline films of other materials.¹¹⁻¹² The HIPIBD process is illustrated in Figure 1. A beam of energetic light ions is deposited over an approximately micron thick ion range, heating the target surface enough to evaporate and ionize material. The resulting energetic plume of ablated material is then condensed as a film onto an adjacent substrate. HIPIBD is similar to PLD and shares many of its advantages, namely: (1) target material stoichiometry is preserved (i.e., the evaporation/deposition is congruent); (2) relatively high-energy ($>5 \text{ eV}$) evaporated species are produced; (3) crucibles and filaments used in thermal evaporation are unnecessary; (4) sequencing with multiple targets is possible; and (5) high instantaneous deposition rates reduce contamination problems. Furthermore, HIPIBD offers several advantages over PLD. Typical ion beams are more energetic and penetrate deeper than conventional laser beams, thereby allowing higher instantaneous evaporation and deposition rates of up to 1 cm/sec .¹¹ Ions also penetrate the surface plasma and couple to the target more efficiently than laser light. Metallic targets, which generally reflect laser light, readily absorb ion beams, allowing for the efficient evaporation of metallic and alloy coatings. HIPIB accelerators have a greater wall-plug efficiency than lasers. All of these factors indicate HIPIBD may be attractive for large scale energetic deposition of materials. Development of a high intensity pulsed ion beam source that will operate at up to 120 Hz is currently underway.¹³

EXPERIMENTAL PROCEDURE

Experiments have been performed on the Los Alamos Anaconda device, a high-intensity pulsed ion beam (HIPIB) accelerator.^{12,14-16} The accelerator consists of a 10-stage Marx generator that can deliver a maximum output pulse of 300 kJ at 1.2 MV. The HIPIB is generated by a magnetically-insulated ion diode attached to the output of the Marx generator. Magnetically-insulated ion diodes are intrinsically high-power-density devices, capable of operating with ion current density enhancement factors orders of magnitude above the Child-Langmuir space-charge limit.¹⁴ The diode used in these experiments consists of an applied-radial magnetic field (B_r) extraction geometry configured for ballistic focusing of the beam as shown in Figure 1. An acrylic dielectric attached to the anode electrode was used as the ion source. The diode was operated at 350 kV, and a maximum ion current of about 35 kA was extracted over the 400 ns pulse. The beam was focused to a 75-mm-diameter "spot", located approximately 300 mm downstream from the diode. Thompson parabola spectrometer measurements revealed a beam primarily composed of carbon ions and protons with particle energies of up to 400 keV.¹⁵ For these experiments, a 203 x 152 x 2.5 mm poco graphite (Union 76 AXF-5Q) target was positioned near the beam focus 25 degrees from the horizontal axis.

The ablated carbon was deposited onto glass substrates that were not preconditioned. The deposition configuration is shown in Figure 1. Two different target/substrate separations were used, 150 and 225 mm. An aluminum substrate holder allowed for deposition of the ablated species onto substrates that were positioned normal to the target and at angles up to 90° off normal to the target (normal position is shown in Fig. 1). Experiments were performed at a base pressure of $\sim 1 \times 10^{-6}$ torr. A base pressure rise up to 200 mtorr from vaporization of the dielectric anode during each pulse was observed, so the deposition chamber required pumping to the base pressure between pulses. The substrates were removed for analysis after approximately 20 pulses.

Film thicknesses were determined by stylus profilometry on substrates which had been masked prior to deposition. Most resistance measurements were carried out using a two point probe, and confirmed with four point measurements. Further film characterization included x-ray

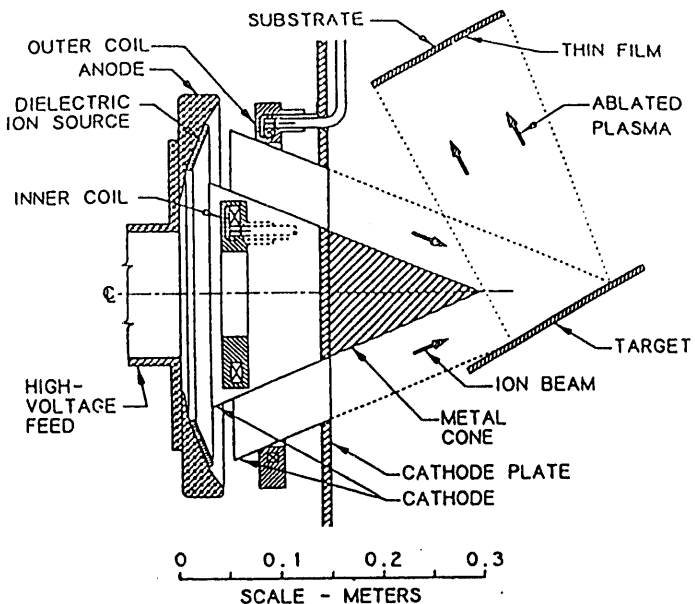


Figure 1. HIPIBD process showing the applied-Br extraction geometry for ballistic focussing.

diffraction (XRD), scanning electron microscopy (SEM), parallel electron energy loss spectroscopy (PEELS), and Raman spectroscopy. SEM was carried out using a 20 keV accelerating voltage. Films were Pt coated by Ar ion sputtering, to prevent charging during analysis. For PEELS, an analytical transmission electron microscope (TEM) was equipped with a magnetic prism spectrometer, which had a parallel detector and was placed below the final viewing screen of the TEM. An accelerating voltage of 200 kV and a spot size of 120 nm were employed. Samples for PEELS were prepared by using 400 mesh copper TEM grids as substrates. These grids were positioned normal to and 225 mm from the target. Deposition was carried out for only two ion beam pulses, producing a thin enough film to minimize multiple inelastic electron scattering events during PEELS. Raman spectrometry was performed using an argon ion laser at 457.9 nm, focused to a ~2 mm x 100 mm line and analyzed using a triple spectrograph/CCD system.

RESULTS AND DISCUSSION

The bulk of the films that were deposited are uniform, light brown, translucent, and dense with some particles in the micron size range. The electrical resistivities are orders of magnitude greater than that of graphite. Significant amounts of sp^3 bonded C was detected by PEELS and Raman spectroscopy.

Each ion beam pulse removed approximately 10 mg of graphite, based on weight measurements before and after 20 shots. This mass removal rate corresponds well to the 7 mg per pulse calculated by an ion beam ablation model. This is a simple thermal model based on the heat conduction equation with mass removal by vaporization only (i.e. no allowance for micron sized particle ejection).¹⁶ Film deposition rates were 25 ± 5 nm per shot onto substrates that were positioned 150 mm from and normal to the target. This rate dropped to about 12 nm per shot at 40° off normal, and at 80° off normal, less than 2 nm per shot was deposited. For the larger target to substrate separation (225 mm), 15 ± 3 nm per shot was deposited normal to the target. This dropped to less than 5 nm/shot at 40° off normal. Based on a 3 μ sec primary ablation pulse as observed by framing photography,¹⁶ instantaneous rates greater than 1 mm/sec were achieved.

JANSEN

6

The films displayed amorphous XRD spectra. Cross sectional SEM micrographs show that the carbon films are uniform with feature sizes of ~100 nm, but large sized particles in the micron size range are present also. Plan views show that the particles range in size from 0.3 to 1.2 μm . There is about ten micron-sized particles per 100 μm^2 .

The electrical resistivities of these films varied from 1 to 1000 $\text{ohm}\cdot\text{cm}$, depending on substrate position relative to the target. The resistivity increased as the target to substrate separation increased. Normal to the target at the shorter target to substrate separation (150 mm), resistivities of the films are ~1 $\text{ohm}\cdot\text{cm}$. However, normal to the target, but 225 mm from the target, the resistivities of the carbon films ranged from 100 to 300 $\text{ohm}\cdot\text{cm}$. As angular offset from the normal increased, resistivities increased to as high as 213 $\text{ohm}\cdot\text{cm}$ for the 150 mm target to substrate separation. For the substrates positioned 225 mm from the target, the resistivities rapidly increased to ~1000 $\text{ohm}\cdot\text{cm}$ as angular offset from the normal increased to 15° and beyond. These resistivities are all orders of magnitude larger than the resistivity of the target, 1×10^{-3} $\text{ohm}\cdot\text{cm}$ at 25°C,¹⁷ and much less than that of pure diamond 1×10^{12} $\text{ohm}\cdot\text{cm}$.¹⁸

PEELS data of a film deposited normal to the target at a distance of 225 mm are shown in Figure 2. The parallel detector used in this experiment allowed all 1024 channels of the spectrum to be detected at once, greatly reducing the acquisition time. This is important, because electron bombardment of DLC reduces the fraction of sp^3 carbon.¹⁹ It has been shown that the electron energy loss corresponding to the K shell ionization is sensitive to the local bonding environment of the carbon atoms.⁹ Two peaks are observed in the C(1s) K absorption edge with maxima at loss energies of about 283 and 291 eV. These features represent transitions from the C(1s) ground state to the π^* and the σ^* conduction bands respectively.²⁰ Assuming the same scattering cross section for the two transitions, the π/σ ratio is quantitatively obtained from the integrated intensities of each peak after background subtraction. Background subtraction was done according to Williams.²¹ For the first peak (283 eV) the pre-edge background, due to the multiply-scattered electrons, was subtracted. For the second peak the pre-edge background, which was subtracted, was due to both the multiply-scattered electrons and the tail of the first peak. Based on this analysis we estimate the π/σ ratio is 1/4. This ratio is 1/3 for sp^2 bonded carbon while sp^3 bonded carbon contains no π bonding. For this film we calculate that 20% of the carbon atoms are sp^3 bonded.

Raman spectra of some of the carbon films are shown in Figure 3. Figure 3(A) and 3(B) are for films deposited at 150 mm from the target. The film of Figure 3(A) was deposited normal to the target and shows Raman bands at 1365 cm^{-1} and 1587 cm^{-1} , that are indicative of glassy carbon (i.e. only sp^2 bonded carbon present). Figure 3(B), deposited 50° off normal, shows these bands as well as an intense band at 1535 cm^{-1} . This band indicates that a significant fraction of the carbon film is diamond like carbon (i.e. an amorphous mixture sp^3 and sp^2 bonded carbon). Figure 3(C) shows data from a film that was deposited 225 mm from and normal to the target. There is only a single band present at 1540 cm^{-1} ; this is the DLC band, but it has been shifted to higher energy. Although Raman Spectroscopy of DLC is not quantitative with regard to sp^3/sp^2 ratio, as the sp^2 bonded carbon fraction increases in the DLC, the Raman shift of the DLC band increases.²² There is no evidence of crystalline diamond, which displays a narrow Raman band at 1330 cm^{-1} , present in any of the spectra.

The lack of DLC in the film deposited normal to and 150 mm from the target, may relate to substrate heating by the depositing species. From framing photography the vaporized plasma (ablation) front expanded at 2 $\text{cm}/\mu\text{sec}$ in an extremely forward directed fashion (normal to the target), analogous to PLD.¹⁶ This velocity corresponds to kinetic energies of 24 eV for atomic carbon. The kinetic energy along with the heat of condensation (7 eV) was released into the substrate upon deposition. At this substrate position about 25 nm of film was deposited per pulse, which corresponds to fluences approaching 1.5 J/cm^2 , depending on the duration of the deposition pulse and the kinetic energy of the depositing species. The extent of substrate heating by the depositing species is currently under investigation. Based on the preliminary results, a

JOHNSON

4

6

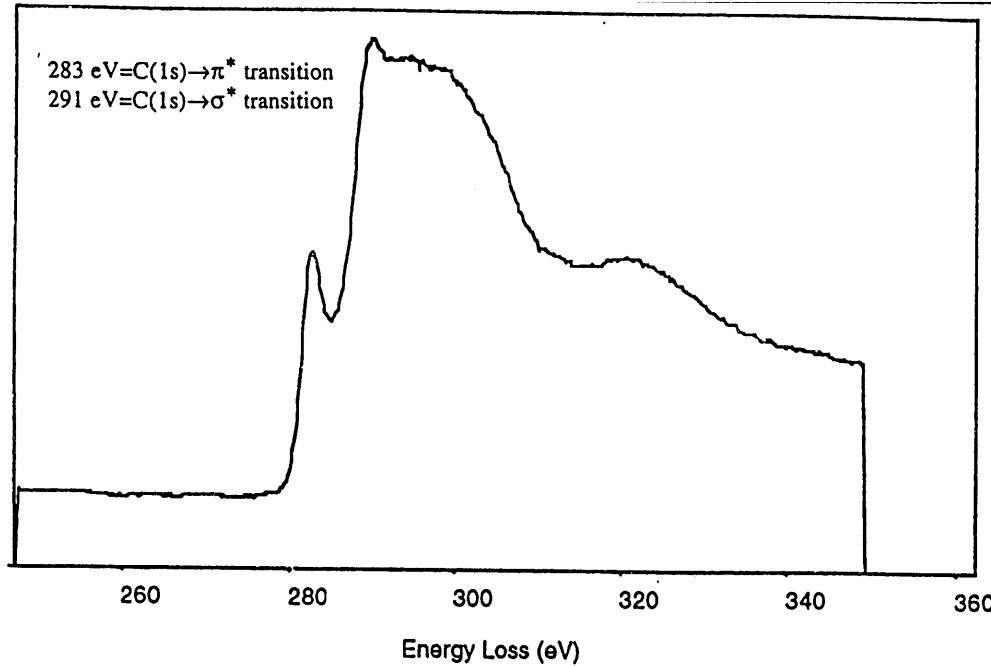


Figure 2. PEELS of DLC Film deposited on a TEM grid for 2 ion beam pulses.

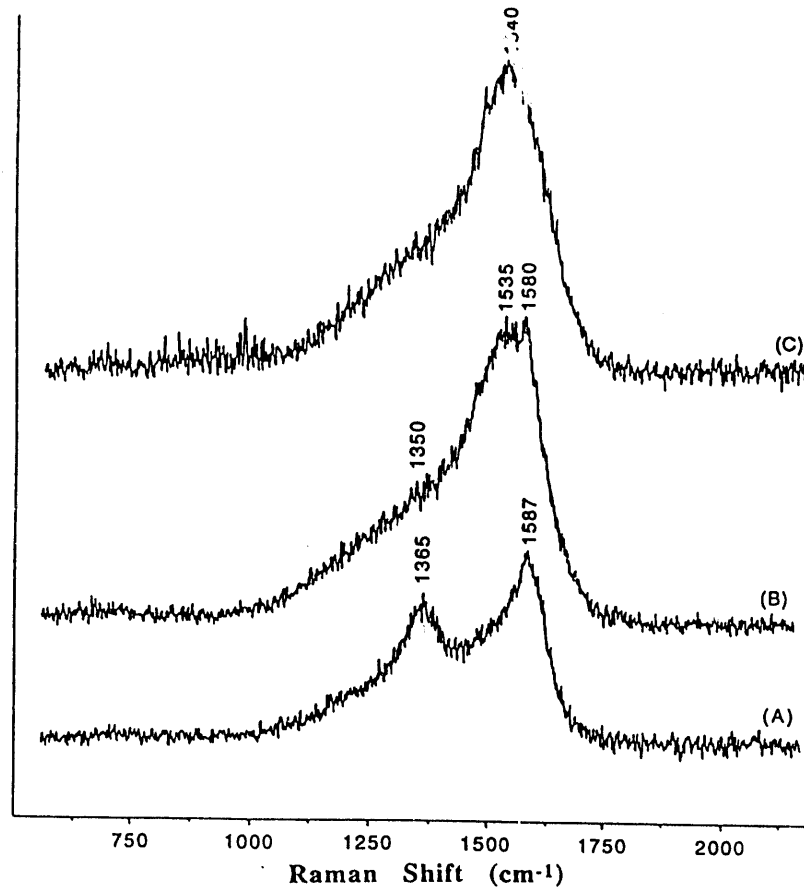


Figure 3. (A) Raman spectra of film deposited at a substrate/target separation of 150 mm and normal to the target. (B) Raman spectra of film deposited at a substrate/target separation of 150 mm and 50° off normal. (C) Raman spectra of film deposited at a substrate/target separation of 225 mm and normal to the target.

Johnson

5

9

glass substrate at this position reaches a temperature of approximately 800°C, which is sufficient heating for rearrangement to the thermodynamically stable sp² bonded carbon.

CONCLUSION

DLC films have been deposited by HIPIBD. Substantial amounts of sp³ bonded carbon were detected by both Raman Spectroscopy and PEELS (up to 20% by PEELS). A highly forward directed ablation plume was observed analogous to PLD. Preliminary evidence indicates that substrate heating by the energetic ablation plume during deposition may reduce the sp³ content of the film. A study of the degree of this substrate heating is underway. Additional studies will probe the effect of substrate pre treatment (etching, both chemical and ion), substrate biasing, and substrate cooling.

REFERENCES

- ¹J. Angus C. Hayman, *Science* **913**, 241 (1988).
- ²D. L. Pappas, K. L. Saenger, J. Bruley, W. Krakow, T. Gu, and W. Collins, *J. Appl. Phys.* **71**(11), 5675 (1992).
- ³J. Robertson, *Phys. Rev. Lett.* **68**, 220 (1992).
- ⁴C. V. Deshpandey and R. F. Bunshah, *J. Vac. Sci. Technol. A* **7**(3), 2294 (1989).
- ⁵S. B. Kim and J. F Wager, *Surface and Coatings Technology* **43/44**, 99 (1990).
- ⁶N. Kumar; U. S. Patent No. 5,199,918 (6 Apr. 1993).
- ⁷D. L. Pappas, K. L. Saenger, J. J. Cuomo, and R. W. Dreyfus, *J. Appl. Phys.* **72**(9), 3966 (1992).
- ⁸J. J. Cuomo, D. L. Pappas, J. Bruley, J. P. Doyle, and K. L. Saenger, *J. Appl. Phys.* **70**(3), 1706 (1991).
- ⁹J. Bruley, J. J. Cuomo, J. P. Doyle, D. L. Pappas, K. L. Saenger, J. C. Liu, and P. E. Batson, *Mater. Res. Soc. Symp. Proc.* **202**, 247 (1991).
- ¹⁰S. Aisenberg and R. Chabot, *J. Appl. Phys.* **42**, 2953 (1971).
- ¹¹Y. Smimotori, M. Yokoyama, H. Isobe, S. Harada, K. Masugata, and K. Yatsui, *J. Appl. Phys.* **63**, 968 (1988).
- ¹²D. C. Gautier, R. E. Muenchhausen, D. J. Rej, B. F. Roberts, G. P. Johnston, W. J. Waganaar, in Beam-Solid Interactions: Fundamentals and Applications, M. Nastasi et al., ed., *MRS Symposium Proc.* **279**, 657 (1993).
- ¹³Harjes et. al., Proceedings of the 8th International Pulsed Power Conference, pp. 543-548, San Diego, 1991.
- ¹⁴D. J. Rej, R. R. Bartsch, H. A. Davis, R. J. Faehl, J. B. Greenly, W. J. Waganaar, *Rev. Sci. Instr.* **64**, 2753 (1993).
- ¹⁵H. A. Davis, submitted to *Rev. Sci. Instr.*
- ¹⁶D. J. Rej, G. P. Johnston, H. A. Davis, R. E. Muenchhausen, C. Ruiz, M. Thompson, and W. J. Waganaar, submitted to *Laser and Particle Beams*.
- ¹⁷W. H. Brixius, Properties and Characterization of Graphite (Poco Graphite, Decatur, Tx., 1987).
- ¹⁸R. M. Chenko and H. M. Strong, General Electric Technical Information Series, Report No. 75CRD089, 1975.
- ¹⁹A. Fuchs, K. Jung H. Ehrhardt, I. Muhling, and K. Breuer, *Thin Solid Films* **217**, 48 (1992).
- ²⁰R. H. Jarman, G. J. Ray, R. W. Standley, and G. W. Zajac, *Appl. Phys. Lett.* **49**(17), 1065 (1986).
- ²¹D. B. Williams, Practical Analytical Electron Microscopy in Materials Science (Philips Electronic Instruments, Mahwah, New Jersey, 1984).
- ²²N. H. Cho, D. K. Veirs, J. W. Ager III, M. D. Rubin, C. B. Hopper, and D. B. Bogy, *J. Appl. Phys.* **71**(5), 2243 (1992).

DISCLAIMER

This report was prepared as an account of work sponsored by an agency of the United States Government. Neither the United States Government nor any agency thereof, nor any of their employees, makes any warranty, express or implied, or assumes any legal liability or responsibility for the accuracy, completeness, or usefulness of any information, apparatus, product, or process disclosed, or represents that its use would not infringe privately owned rights. Reference herein to any specific commercial product, process, or service by trade name, trademark, manufacturer, or otherwise does not necessarily constitute or imply its endorsement, recommendation, or favoring by the United States Government or any agency thereof. The views and opinions of authors expressed herein do not necessarily state or reflect those of the United States Government or any agency thereof.

6
3
1811
DEMENTED
DATE



